



## Evaluating Electrolyte Solvent Effects on Low-Temperature Performance of Lithium-ion Batteries Using Electrochemical Impedance Spectroscopy

Mohammad Zarei-Jelyani<sup>1\*</sup>, Amirhossein Salehi<sup>1</sup>, Mohsen Babaiee<sup>1</sup>, Mohammad Mohsen Loghavi<sup>1</sup>

<sup>1</sup>Department of Energy Storage, Institute of Mechanics, Shiraz, Iran

### ARTICLE INFO

#### Article history:

Received : 19 Jan 2024

Accepted: 30 Mar 2024

Published: 21 Apr 2024

#### Keywords:

Li-ion battery

Electrolyte

Solvent

Low-temperature performance

Impedance spectroscopy

### ABSTRACT

The global transition towards renewable energy necessitates efficient energy storage solutions to address the intermittency of renewable sources like solar and wind power. Lithium-ion batteries (LIBs), widely utilized in electric vehicles (EVs) for their high energy density and efficiency, have emerged as a leading technology, yet their performance at low temperatures remains a challenge. This study investigates the influence of electrolyte solvent composition on LIB performance under low-temperature conditions using electrochemical impedance spectroscopy (EIS). Three electrolytes were studied: a standard electrolyte (STDE) comprising 1 M LiPF<sub>6</sub> in ethylene carbonate (EC) and diethyl carbonate (DEC), a low-temperature electrolyte (LTE) consisting of 1 M LiPF<sub>6</sub> in EC, ethyl methyl carbonate (EMC), and ethyl acetate (EA), and a long-cycle-life electrolyte (LCLE) containing 1 M LiPF<sub>6</sub> in EC/EMC. The EIS results revealed significant differences in resistance values among the electrolytes at varying temperatures. Specifically, at 0 °C, the STDE exhibited a charge transfer resistance ( $R_{ct}$ ) of 1055.3  $\Omega$  and a solid electrolyte interface resistance ( $R_{SEI}$ ) of 803.4  $\Omega$ , whereas the LTE showed a substantially lower  $R_{ct}$  of 507.4  $\Omega$  and  $R_{SEI}$  of 64.2  $\Omega$ , indicating superior low-temperature performance. Similarly, at -20 °C, the  $R_{ct}$  values for STDE, LTE, and LCLE were 8878.6  $\Omega$ , 854.2  $\Omega$ , and 15622  $\Omega$ , respectively, with corresponding  $R_{SEI}$  values of 172.1  $\Omega$ , 92.4  $\Omega$ , and 2364  $\Omega$ . These findings underscore the importance of solvent composition in mitigating resistance increases at lower temperatures and highlight the superior performance of the LTE formulation in maintaining lower  $R_{ct}$  and  $R_{SEI}$  values. Notably, the addition of ethyl acetate (EA) in the LTE formulation contributed to enhanced low-temperature performance, likely by lowering the overall viscosity of the electrolyte mixture and improving ionic mobility. This study demonstrates the critical role of solvent composition, particularly EA, in optimizing LIB performance for cold climate applications.

## 1. Introduction

The global energy landscape is undergoing a transformative shift from fossil fuels to renewable energy sources, driven by the urgent need to combat climate change and ensure sustainable energy security [1-4]. Renewable energy sources

like solar, wind, hydro, and geothermal are abundant, sustainable, and emit little to no greenhouse gases. However, these sources face inherent challenges due to their intermittent and variable nature. Solar and wind power generation, for instance, are dependent on weather conditions

\*Mohammad Zarei-Jelyani

Email Address: zjmohammad.ui@gmail.com

<https://doi.org/10.22068/ase.2024.672>

and time of day, leading to fluctuations in energy supply. This variability necessitates reliable and efficient energy storage solutions to ensure a stable and continuous power supply. Energy storage systems (ESS) are pivotal in balancing supply and demand, enhancing grid stability, and optimizing the utilization of renewable energy [5-8].

Batteries, particularly lithium-ion batteries (LIBs), have emerged as a leading technology in energy storage due to their high energy density, long cycle life, low self-discharge rates, and high efficiency [9-11]. LIBs have revolutionized portable electronics and electric vehicles (EVs) and are increasingly being integrated into grid storage systems [12-17]. Despite their advantages, LIBs face significant performance challenges at low temperatures. Cold environments, especially sub-zero temperatures, can drastically impair the performance of LIBs by reducing their capacity, power output, and overall efficiency. This limitation is critical for applications in cold climates and high-altitude regions, as well as for certain aerospace applications where reliable battery performance is essential regardless of the ambient temperature [18-22].

The properties of the electrolyte heavily influence the performance of LIBs in low-temperature conditions. The electrolyte in a LIB serves as a medium for ion transport between the cathode and anode during the charge and discharge processes. It typically consists of a lithium salt dissolved in a solvent or a mixture of solvents and may also include co-solvents and additives to enhance performance [23, 24]. Lithium salts are a crucial component of the electrolyte, providing the necessary lithium ions for conduction. Due to its good ionic conductivity and stable electrochemical performance,  $\text{LiPF}_6$  salt finds widespread use, despite its susceptibility to moisture and potential for decomposition at high temperatures.

Lithium bis(trifluoromethane)sulfonimide ( $\text{LiTFSI}$ ) salt is more expensive and can damage aluminum current collectors, but it is better at low temperatures and has better thermal and chemical stability than  $\text{LiPF}_6$ . It also conducts ions more efficiently [25, 26].

The choice of solvent significantly affects the electrolyte's properties, including its viscosity, dielectric constant, and electrochemical stability. Common solvents used in LIB electrolytes include ethylene carbonate (EC), dimethyl carbonate (DMC), and propylene carbonate (PC).

Co-solvents are often added to the electrolyte to optimize performance by balancing the properties of the primary solvents. For instance, ethyl methyl carbonate (EMC) is often used alongside EC and DMC to improve low-temperature performance and reduce viscosity. Diethyl carbonate (DEC) helps to lower the freezing point of the electrolyte and reduce its viscosity [27].

Additives play a crucial role in enhancing the performance and safety of LIB electrolytes. They can improve the formation and stability of the solid electrolyte interphase (SEI) layer, enhance ionic conductivity, and increase the overall electrochemical stability of the electrolyte. For example, vinylene carbonate (VC) is known for improving the stability of the SEI layer and enhancing battery life [28]. Fluoroethylene carbonate (FEC) enhances low-temperature performance and the stability of the SEI layer, especially for silicon-based anodes [29, 30]. Lithium difluoro(oxalato)borate ( $\text{LiDFOB}$ ) is used to improve thermal stability and reduce the risk of thermal runaway [31, 32].

In the context of low-temperature performance, electrochemical impedance spectroscopy (EIS) can reveal critical information about the increased resistance and reduced ion mobility that affect battery performance. By systematically analyzing different electrolyte formulations through EIS, researchers can develop strategies to optimize electrolyte composition, enhancing the low-temperature performance of LIBs [33, 34]. This approach is essential for advancing battery technologies that can reliably operate in diverse and extreme environmental conditions, supporting the broader integration of renewable energy systems across various geographic and climatic regions.

The present study investigates the effect of electrolyte solvent composition on the electrochemical performance of lithium-ion batteries under low temperature conditions, utilizing the EIS technique. The three investigated electrolytes consist of  $\text{LiPF}_6$  salt dissolved in various solvents, including EC/DEC, EC/EMC, and EC/EMC/EA.

## 2. Experimental

### 2.1. Cathode electrode preparation

The cathode electrode was fabricated utilizing the active constituent of nickel manganese cobalt oxide (NMC, Targray group). The conductive agent employed in the cathodes was carbon black

C45, manufactured by Imerys Company. The binder solution was produced by incorporating N-Methyl-Pyrrolidone (NMP, Scharlau Company), a solvent, and polyvinylidene fluoride (PVDF) from the Arkema group. The process of surface modification of aluminum foil was carried out with cold plasma. Subsequently, the aluminum foil was appropriately dimensioned. The cathode slurries were applied to aluminum current collectors using a blade gap of 80  $\mu\text{m}$  at a speed of 10  $\text{m min}^{-1}$ . Afterwards, the electrodes underwent a drying process within a vacuum oven for a duration of 20 hours, keeping a temperature of 60  $^{\circ}\text{C}$ .

## 2.2. Coin cell assembly

The CR2032 coin-type half-cells, consisting of two electrodes, were manufactured in a glove box with controlled moisture and oxygen levels, both kept below 0.5 ppm. A porous polypropylene film served as the separator for all cells. Three distinct cathode half-cells were produced, with each one using a different electrolyte. An NMC cathode electrode was used as the working electrode (positive side). Lithium metal foil, with a diameter of 16 mm and a thickness of 0.6 mm, served as both the counter and reference electrode (negative side). Three different kinds of electrolytes were employed: a standard electrolyte (STDE), a low-temperature electrolyte (LTE), and a long-cycle-life electrolyte (LCLE). The STDE, obtained from MTI Corporation, was 1 M  $\text{LiPF}_6$  in EC/DEC (1:1). The LTE, provided by Dongguan Shanshan Battery Material Co., Ltd., consisted of 1 M  $\text{LiPF}_6$  in EC/EMC (3:7) with Ethyl Acetate (EA). The LCLE, sourced from Gelon, consisted of 1 M  $\text{LiPF}_6$  in EC/EMC (1:1).

An electric coin cell crimping machine was used to crimp the coin cells, ensuring a strong seal. Following the assembly process, a 24-hour resting period was given for the cells. The resting time ensured that the electrolyte percolated thoroughly across the separator's pores, which is critical for the cell's effective operation.

## 2.3. Characterization

The formation of coin cells was carried out through five charge-discharge cycles within the voltage range of 2.8 to 4.2 V. The charging procedure was conducted using the constant current-constant voltage (CC-CV) method, with a current of 20  $\text{mA g}^{-1}$  (about 0.1C) and a cut-off current of 4  $\text{mA g}^{-1}$ . The cells were discharged with a current of 20  $\text{mA g}^{-1}$ . The battery test

system (BTS 8000, Neware Ltd.) was used to perform the formation charge and discharge cycles. The formation data were obtained at ambient pressure and also at a temperature of 25  $^{\circ}\text{C}$  set by a temperature control chamber. Following the formation process, the electrochemical impedance spectrometry (EIS) tests were conducted in a fully charged state. The experiments were carried out within a frequency range of 100 kHz to 10 mHz at temperatures of 25, 0, -20, and -40  $^{\circ}\text{C}$ . The Autolab PGSTAT302N, which is galvanostat and potentiostat equipment, was employed for conducting EIS experiments.

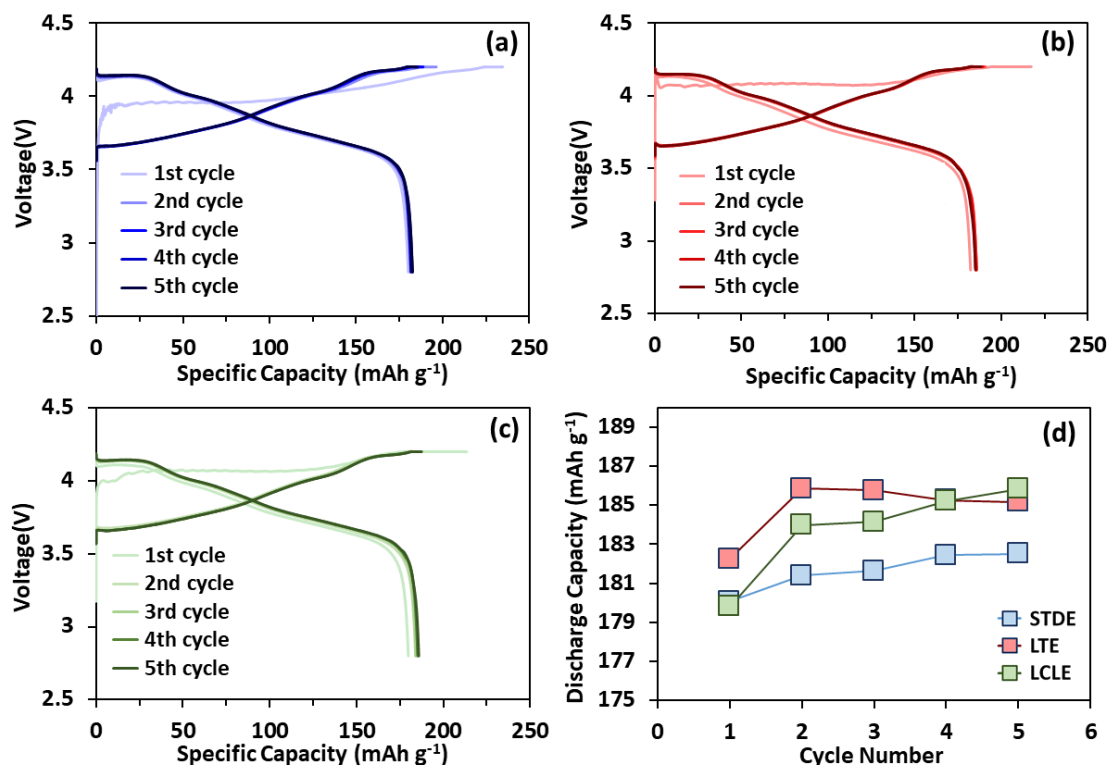
## 3. Results and discussion

Figure 1(a)–(c) and Figure 1(d) show the charge-discharge profiles and discharge capacity diagrams during the five-cycle electrochemical formation of coin cells, respectively. For all three types of electrolytes, the overall appearance of the charge-discharge profiles is the same. The curve of the first charge had a higher voltage level than the subsequent charge curves that overlapped during the next 4 cycles. Most of the electrochemical formation process takes place during the first charge. For the case of LTE, the charging voltage was started above 4 V in the first cycle, while for the other two cases, it was below 4 V. The LTE exhibited a distinct behavior in the first charge due to the presence of EA in its formulation. The inclusion of EA likely reduced the overall viscosity of the electrolyte, enhancing ionic mobility. This improvement in ionic transport could explain why the LTE started with a higher voltage above 4 V during the first charge, compared to the other electrolytes. The lower viscosity and better ionic conductivity facilitated a more efficient electrochemical formation process, leading to a different charging profile.

According to the discharge curves, the average discharge voltage during 5 cycles for all three cases was close to each other, so it was 3.85 V for the STDE and 3.84 V for the other ones. According to Figure 1(d), the discharge capacity increased gradually from the first to the fifth cycle of formation for STDE and LCLE, while for the LTE sample, it first increased and then stabilized. Based on the averaging of the discharge capacities obtained during 5 formation cycles, the LTE sample provided the highest value (184.9  $\text{mAh g}^{-1}$ ) and the STDE sample had the lowest capacity (181.6  $\text{mAh g}^{-1}$ ). Higher capacity in LTE compared to STDE and LCLE can be attributed to the superior ionic conductivity provided by

the EA in the electrolyte, which helps maintain lower resistance and stable

electrochemical reactions during discharge.



**Figure 1:** Charge-discharge profiles of (a) STDE, (b) LTE, and (c) LCLE; and (d) discharge capacity diagrams during the five-cycle electrochemical formation.

The Nyquist diagrams at different temperatures of 25, 0, -20, and -40 °C for the half-cells assigned STDE, LTE, and LCLE are depicted in Figure 2. The corresponding equivalent circuit is illustrated as well in Figure 3(a). The  $R_o$  represents the resistance of the bulk electrolyte, whereas the parallel circuit of  $R_{cc}||CPE_{cc}$  is responsible for the current conduction among the electrode and current collector. The subsequent parallel circuit ( $R_{SEI}||CPE_{SEI}$ ) indicates the influence of the SEI film on the impedance's middle frequency range. The  $R_{ct}||CPE_{ct}$  parallel circuit represents the charge transfer resistance during the intercalation process across the electrodes and electrolyte. The slope of the line at low frequencies refers to the Warburg impedance, which denotes the diffusion of  $Li^+$  ions at the boundary between the electrode and electrolyte. Table 1 and Figure 3 show the

results of simulations derived from EIS data for different electrolytes at various temperatures.

The standard electrolyte (STDE), which consists of 1 M LiPF<sub>6</sub> in EC/DEC (1:1), exhibited significant increases in various resistances as the temperature decreased. At 25 °C, the  $R_{ct}$  was 96.4 Ω and the  $R_{SEI}$  was 116.1 Ω, indicating reasonable performance under standard conditions. However, at 0 °C, the  $R_{ct}$  increased to 1055.3 Ω and  $R_{SEI}$  to 803.4 Ω, reflecting a significant drop in performance. At -20 °C, these values surged to 8878.6 Ω and 172.1 Ω, respectively, and at -40 °C, the  $R_{ct}$  reached a staggering 20755 Ω with the  $R_{SEI}$  at 1799 Ω. These results indicate that the STDE's performance severely deteriorates at lower temperatures due to the increased viscosity of the EC/DEC mixture, which hinders ionic mobility and increases resistance.

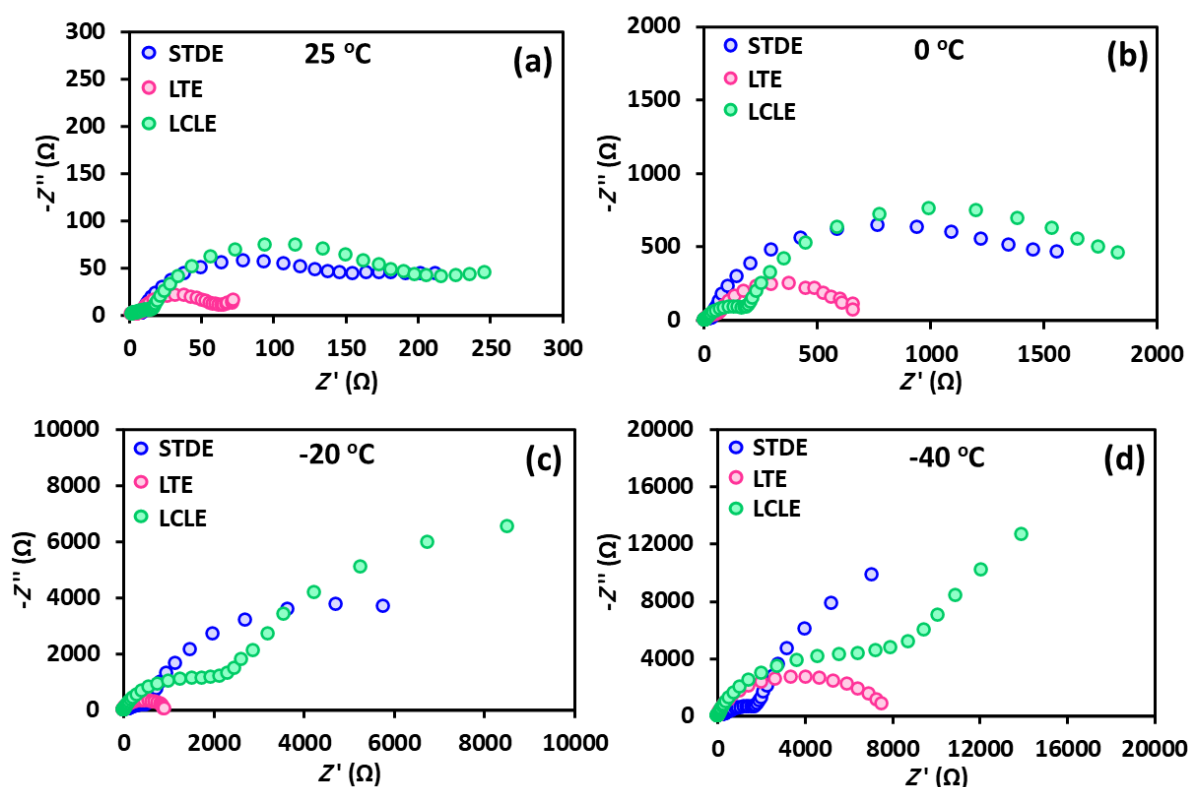


**Figure 2:** The Nyquist diagrams at different temperatures of 25, 0, -20, and -40 °C for the half-cells assigned STDE, LTE, and LCLE.

In contrast, the LTE, formulated with 1 M LiPF<sub>6</sub> in EC/EMC (3:7) and ethyl acetate (EA), demonstrated superior low-temperature performance. At 25 °C, the  $R_{ct}$  was a mere 3.6  $\Omega$ , and the  $R_{SEI}$  was 48.8  $\Omega$ , which are significantly lower than those of the STDE, indicating excellent ionic conductivity. Even at 0 °C, the LTE maintained a  $R_{ct}$  of 507.4  $\Omega$  and an  $R_{SEI}$  of 64.2  $\Omega$ . At -20 °C, the  $R_{ct}$  remained manageable at 854.2  $\Omega$  and the  $R_{SEI}$  at 92.4  $\Omega$ . Finally, at -40 °C, although the resistances increased to 5709  $\Omega$  for  $R_{ct}$  and 1346  $\Omega$  for  $R_{SEI}$ , they were still substantially lower than those of the STDE. The superior performance of the LTE at low temperatures can be attributed to the presence of EA, which helps to lower the overall viscosity of the electrolyte mixture and enhance ionic mobility even at sub-zero temperatures.

The LCLE, composed of 1 M LiPF<sub>6</sub> in EC/EMC (1:1), showed the highest  $R_{ct}$  values across all temperatures, indicating poor performance in low-temperature conditions. At 25 °C,  $R_{ct}$  was 140.8  $\Omega$  and  $R_{SEI}$  was 136  $\Omega$ ,

already higher than the other electrolytes. As the temperature dropped to 0 °C,  $R_{ct}$  increased to 1369.1  $\Omega$  and  $R_{SEI}$  to 172.1  $\Omega$ . At -20 °C, these values soared to 15622  $\Omega$  for  $R_{ct}$  and 2364  $\Omega$  for  $R_{SEI}$ . At -40 °C, the LCLE displayed the highest resistances among all tested electrolytes, with  $R_{ct}$  at 24486  $\Omega$  and  $R_{SEI}$  at 7530  $\Omega$ . The poor performance of the LCLE at low temperatures can be explained by the higher viscosity of the EC/EMC (1:1) mixture, which significantly impedes ionic transport and increases resistance.

A comparative analysis of the solvents EMC and DEC based on the EIS results reveals that EMC, particularly when combined with EA, offers superior low-temperature performance compared to DEC. The LTE with EMC and EA showed consistently lower  $R_{ct}$  and  $R_{SEI}$  values across all temperatures tested, indicating better ionic conductivity and lower impedance. The DEC-containing STDE, on the other hand, exhibited a dramatic increase in resistance as the temperature dropped, highlighting the limitations of DEC in low-temperature applications.

Evaluating Electrolyte Solvent Effects on Low-Temperature Performance of Lithium-ion Batteries Using Electrochemical Impedance Spectroscopy

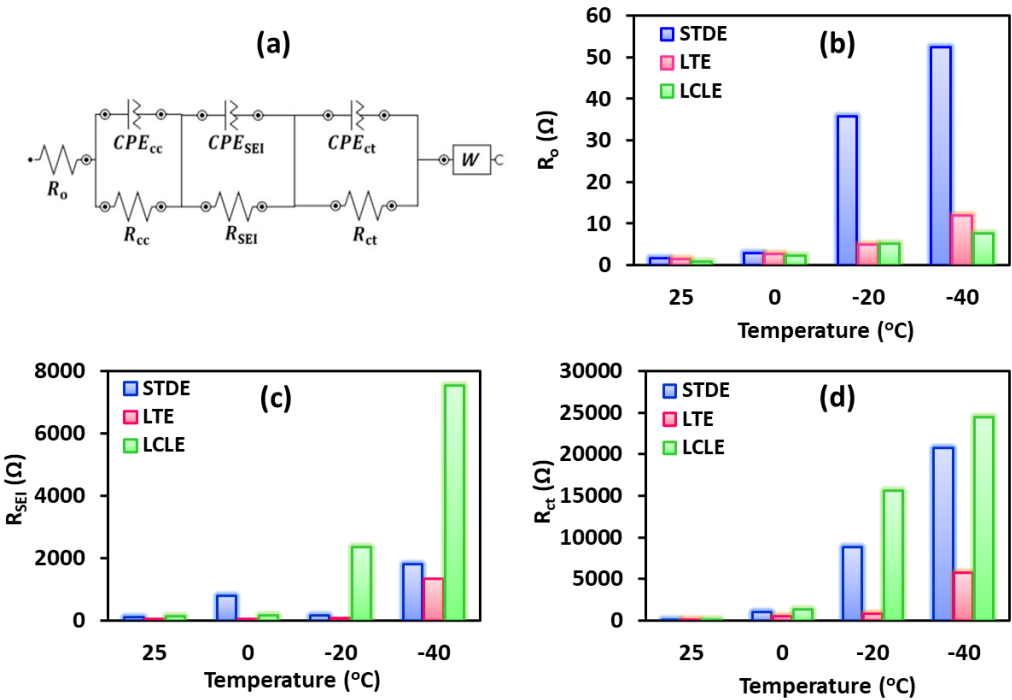


Figure 3: The corresponding equivalent circuit (a) and the results of simulations derived from EIS data for STDE, LTE, and LCLE half-cells at various temperatures (b, c, and d).

Table 1: The results of simulations derived from EIS data for different electrolytes at various temperatures.

Temperature (°C)	Electrolyte	$R_0$ (Ω)	$R_{cc}$ (Ω)	$R_{SEI}$ (Ω)	$R_{ct}$ (Ω)
25	STDE	1.65	7.57	116.07	96.46
	LTE	1.47	3.36	48.83	3.62
	LCLE	0.86	21.39	136.04	140.81
0	STDE	2.81	47.72	803.45	1055.32
	LTE	2.78	4.09	64.18	507.38
	LCLE	2.23	11.69	172.07	1369.11
-20	STDE	35.74	341.42	172.11	8878.61
	LTE	4.88	5.51	92.43	854.17
	LCLE	5.08	28.75	2364.03	15622.25
-40	STDE	52.44	801.07	1799.21	20755.36
	LTE	11.86	14.29	1346.91	5709.73
	LCLE	7.63	29.11	7530.62	24486.47

#### 4. Conclusions

This study elucidates the pivotal role of electrolyte solvent composition in shaping the low-temperature performance of LIBs. Three electrolytes were studied: a standard electrolyte comprising 1 M LiPF<sub>6</sub> in EC/DEC, a low-temperature electrolyte consisting of 1 M LiPF<sub>6</sub> in EC/EMC/EA, and a long-cycle-life electrolyte containing 1 M LiPF<sub>6</sub> in EC/EMC. The results underscore significant differences in resistance values among the electrolytes at varying temperatures, highlighting the critical influence of solvent composition on LIB performance. At 0 °C, the STDE exhibited a  $R_{ct}$  of 1055.3  $\Omega$  and a  $R_{SEI}$  of 803.4  $\Omega$ , while the LTE demonstrated substantially lower  $R_{ct}$  (507.4  $\Omega$ ) and  $R_{SEI}$  (64.2  $\Omega$ ), indicative of superior low-temperature performance. Similarly, at -20 °C, the  $R_{ct}$  values for STDE, LTE, and LCLE were 8878.6  $\Omega$ , 854.2  $\Omega$ , and 15622  $\Omega$ , respectively, with corresponding  $R_{SEI}$  values of 172.1  $\Omega$ , 92.4  $\Omega$ , and 2364  $\Omega$ . Furthermore, at -40 °C, the resistance values followed a similar trend, emphasizing the superior performance of the LTE formulation. The addition of ethyl acetate (EA) in the LTE formulation played a crucial role in enhancing low-temperature performance by potentially reducing viscosity and improving ionic mobility. This finding shows the importance of solvent composition, particularly the inclusion of EA, in optimizing LIB performance for cold climates and extreme environmental conditions. The results have significant implications for the application of LIBs in battery electric vehicles (BEVs) and hybrid electric vehicles (HEVs). By maintaining lower resistance and higher ionic mobility at sub-zero temperatures, the LTE formulation can enhance the efficiency and reliability of LIBs in BEVs and HEVs, especially in regions with harsh winters. This improvement aligns with the global transition towards renewable energy and electric mobility, as discussed in the introduction. Optimizing electrolyte formulations for low-temperature performance is crucial for extending the range, lifespan, and overall performance of electric vehicles, thereby supporting broader

adoption and integration of renewable energy solutions.

#### Declaration of Conflicting Interests

The authors declared no potential conflicts of interest with respect to the research, authorship, and publication of this article.

#### Acknowledgements

The authors would like to express their gratitude to the Institute of Mechanics for financial support.

#### References

- [1] M. Zarei-Jelyani, M. Babaiee, S. Baktashian, and R. Egra, "Unraveling the role of binder concentration on the electrochemical behavior of mesocarbon microbead anode in lithium-ion batteries: understanding the formation of the solid electrolyte interphase", *Journal of Solid State Electrochemistry*, Vol. 23, No. 10, (2019), pp. 2771-2783.
- [2] K. Xu, "A long journey of lithium: from the big bang to our smartphones", *Energy & Environmental Materials*, Vol. 2, No. 4, (2019), pp. 229-233.
- [3] F. Zarei-Jelyani, F. Salahi, M. Zarei-Jelyani, and M. R. Rahimpour, "Various Industrial Wastes to Energy Technologies". *Reference Module in Earth Systems and Environmental Sciences*, Elsevier (2024).
- [4] A. Salehi *et al.*, "Facile synthesis of hierarchical porous Na<sub>3</sub>V<sub>2</sub>(PO<sub>4</sub>)<sub>3</sub>/C composites with high-performance Na storage properties", *Journal of Power Sources*, Vol. 481, (2021) p. 228828.
- [5] B. Dunn, H. Kamath, and J.-M. Tarascon, "Electrical energy storage for the grid: a battery of choices", *Science*, Vol. 334, No. 6058, (2011), pp. 928-935.
- [6] M. Zarei-Jelyani, F. Zarei-Jelyani, F. Salahi, and M. R. Rahimpour, "Wind Distributed Generation System".



- Reference Module in Earth Systems and Environmental Sciences*, Elsevier (2024).
- [7] G. Zhu *et al.*, "Materials insights into low-temperature performances of lithium-ion batteries", *Journal of Power Sources*, Vol. 300, (2015), pp. 29-40.
  - [8] M. Zarei-Jelyani, M. M. Loghavi, M. Babaiee, and R. Egra, "Comparative analysis of single-acid and mixed-acid systems as supporting electrolyte for vanadium redox flow battery", *Journal of Applied Electrochemistry*, Vol. 54, No. 4, (2024), pp. 719-730.
  - [9] M. Babaiee, M. Zarei-Jelyani, S. Baktashian, and R. Egra, "Surface modification of copper current collector to improve the mechanical and electrochemical properties of graphite anode in lithium-ion battery", *Journal of Renewable Energy and Environment*, Vol. 9, No. 1, (2022), pp. 63-69.
  - [10] M. M. Loghavi, M. Babaiee, and R. Egra, "A review of volumetric titration as an efficient method for the quantification of ions and compounds in lithium-ion battery components", *Chemical Papers*, Vol. 77, No. 12, (2023), pp. 7395-7408.
  - [11] A. Yaghtin, S. M. Masoudpanah, M. Hasheminasari, A. Salehi, D. Safanama, C. K. Ong, S. Adams, and M. V. Reddy, "Effect of reducing agent on solution synthesis of  $\text{Li}_3\text{V}_2(\text{PO}_4)_3$  cathode material for lithium ion batteries", *Molecules*, Vol. 25, No. 16, (2020), p. 3746.
  - [12] Y. Liu, R. Zhang, J. Wang, and Y. Wang, "Current and future lithium-ion battery manufacturing", *IScience*, Vol. 24, No. 4, (2021).
  - [13] Y. Zheng, Y. Yao, J. Ou, M. Li, D. Luo, H. Dou, Z. Li, K. Amine, A. Yu, and Z. Chen, "A review of composite solid-state electrolytes for lithium batteries: fundamentals, key materials and advanced structures", *Chemical Society Reviews*, Vol. 49, No. 23, (2020), pp. 8790-8839.
  - [14] M. Babaiee, S. Baktashian, M. Zarei-Jelyani, R. Egra, and M. Gholami, "High-Performance Natural Graphite Anode for Lithium-Ion Batteries: Using  $\text{TiO}_2$  as an Additive", *ChemistrySelect*, Vol. 7, No. 29, (2022), p. e202201510.
  - [15] L. Li, D. Zhang, J. Deng, Y. Gou, J. Fang, H. Cui, Y. Zhao, and M. Cao, "Carbon-based materials for fast charging lithium-ion batteries", *Carbon*, Vol. 183, (2021), pp. 721-734.
  - [16] M. Zarei-Jelyani and F. Esmaeilzadeh, "A semi-empirical and multi-variable model for prediction of capacity loss in lithium-ion batteries: Considering cycling and performance time degradations", *Journal of Power Sources*, Vol. 602, (2024), p. 234377.
  - [17] M. Sarshar, M. Zarei-Jelyani, and M. Babaiee, "Application of semi empirical and multiphysics models in simulating lithium ion battery operation", in *10th International Chemical Engineering Congress and Exhibition (IChEC 2018)*, Isfahan, Iran, 2018.
  - [18] J. Fan and S. Tan, "Studies on charging lithium-ion cells at low temperatures", *Journal of The Electrochemical Society*, Vol. 153, No. 6, (2006), p. A1081.
  - [19] A. Laforge, X. Z. Yuan, A. Platt, S. Brueckner, F. Perrin-Sarazin, M. Toupin, J. Y. Huot, and A. Mokrini, "Effects of fast charging at low temperature on a high energy Li-ion battery", *Journal of the electrochemical society*, Vol. 167, No. 14, (2020), p. 140521.
  - [20] K. Bi, S.-X. Zhao, C. Huang, and C.-W. Nan, "Improving low-temperature performance of spinel  $\text{LiNi}_0.5\text{Mn}_{1.5}\text{O}_4$  electrode and  $\text{LiNi}_{0.5}\text{Mn}_{1.5}\text{O}_4/\text{Li}_4\text{Ti}_5\text{O}_{12}$  full-cell by coating solid-state electrolyte  $\text{Li-Al-Ti-PO}$ ", *Journal of Power Sources*, Vol. 389, (2018), pp. 240-248.
  - [21] M. Zarei-Jelyani, M. Babaiee, S. Baktashian, R. Egra, and H. Shirani-Faradonbeh, "Assessment of the formation process effect on the lithium-ion battery performance at low temperatures", *Journal of Materials Science: Materials in Electronics*, Vol. 34, No. 27, (2023), p. 1890.
  - [22] Y. Na, X. Sun, A. Fan, S. Cai, and C. Zheng, "Methods for enhancing the capacity of electrode materials in low-



- temperature lithium-ion batteries", *Chinese Chemical Letters*, Vol. 32, No. 3, (2021), pp. 973-982.
- [23] K. Hayashi, Y. Nemoto, S.-i. Tobishima, and J.-i. Yamaki, "Mixed solvent electrolyte for high voltage lithium metal secondary cells", *Electrochimica Acta*, Vol. 44, No. 14, (1999), pp. 2337-2344.
- [24] M. Ding, K. Xu, S. Zhang, K. Amine, G. Henriksen, and T. Jow, "Change of conductivity with salt content, solvent composition, and temperature for electrolytes of LiPF<sub>6</sub> in ethylene carbonate-ethyl methyl carbonate", *Journal of the Electrochemical Society*, Vol. 148, No. 10, (2001), p. A1196.
- [25] S. E. Sloop, J. K. Pugh, S. Wang, J. B. Kerr, and K. Kinoshita, "Chemical reactivity of PF<sub>5</sub> and LiPF<sub>6</sub> in ethylene carbonate/dimethyl carbonate solutions", *Electrochemical and Solid-State Letters*, Vol. 4, No. 4, (2001), p. A42.
- [26] H.-B. Han, S. S. Zhou, D. J. Zhang, S. W. Feng, L. F. Li, K. Liu, W. F. Feng, J. Nie, H. Li, X. J. Huang, and M. Armand, "Lithium bis (fluorosulfonyl) imide (LiFSI) as conducting salt for nonaqueous liquid electrolytes for lithium-ion batteries: Physicochemical and electrochemical properties", *Journal of Power Sources*, Vol. 196, No. 7, (2011), pp. 3623-3632.
- [27] W. Lin, M. Zhu, Y. Fan, H. Wang, G. Tao, M. Ding, N. Liu, H. Yang, J. Wu, J. Fang, and Y. Tang, "Low temperature lithium-ion batteries electrolytes: Rational design, advancements, and future perspectives", *Journal of Alloys and Compounds*, Vol. 905, (2022), p. 164163.
- [28] R. Lundström, N. Gogoi, T. Melin, and E. J. Berg, "Unveiling Reaction Pathways of Ethylene Carbonate and Vinylene Carbonate in Li-Ion Batteries", *The Journal of Physical Chemistry C*, (2024).
- [29] L. Liao, X. Cheng, Y. Ma, P. Zuo, W. Fang, G. Yin, and Y. Gao, "Fluoroethylene carbonate as electrolyte additive to improve low temperature performance of LiFePO<sub>4</sub> electrode", *Electrochimica Acta*, Vol. 87, (2013), pp. 466-472.
- [30] E. Markevich, G. Salitra, and D. Aurbach, "Fluoroethylene carbonate as an important component for the formation of an effective solid electrolyte interphase on anodes and cathodes for advanced Li-ion batteries", *ACS Energy Letters*, Vol. 2, No. 6, (2017), pp. 1337-1345.
- [31] H. Xiang, P. Shi, P. Bhattacharya, X. Chen, D. Mei, M. E. Bowden, J. Zheng, J. G. Zhang, and W. Xu, "Enhanced charging capability of lithium metal batteries based on lithium bis (trifluoromethanesulfonyl) imide-lithium bis (oxalato) borate dual-salt electrolytes", *Journal of Power Sources*, Vol. 318, (2016), pp. 170-177.
- [32] X. Chen, W. Xu, M. H. Engelhard, J. Zheng, Y. Zhang, F. Ding, J. Qian, and J. G. Zhang, "Mixed salts of LiTFSI and LiBOB for stable LiFePO<sub>4</sub>-based batteries at elevated temperatures", *Journal of Materials Chemistry A*, Vol. 2, No. 7, (2014), pp. 2346-2352.
- [33] X. H. Ma, X. Cao, Y. Y. Ye, F. Qiao, M. F. Qian, Y. Y. Wei, Y. D. Wu, Z. F. Zi, and J. M. Dai, "Study on low-temperature performances of Nb<sub>16</sub>W<sub>5</sub>O<sub>55</sub> anode for lithium-ion batteries", *Solid State Ionics*, Vol. 353, (2020), p. 115376.
- [34] M. Smart, B. Ratnakumar, and S. Surampudi, "Use of organic esters as cosolvents in electrolytes for lithium-ion batteries with improved low temperature performance", *Journal of the Electrochemical Society*, Vol. 149, No. 4, (2002), p. A361.